Appl Phys B (2008) 93: 907–914
DOI 10.1007/s00340-008-3271-4

Applied Physics B
Lasers and Optics

Diode laser atomic fluorescence temperature measurements in low-pressure flames

I.S. Burns · N. Lamoureux · C.F. Kaminski · J. Hult · P. Desgroux

Received: 10 April 2008 / Revised version: 10 September 2008 / Published online: 31 October 2008

Abstract Temperature measurements have been performed in a low-pressure flame by the technique of diode laser induced atomic fluorescence. The experiments were done in a near-stoichiometric flat-flame of premixed methane, oxygen and nitrogen, at a pressure of 5.3 kPa. Indium atoms were seeded to the flame and probed using blue diode lasers; the lineshapes of the resulting fluorescence spectra were used to determine the flame temperature at a range of heights above the burner plate. The particular issues associated with the implementation of this measurement approach at low pressure are discussed, and it is shown to work especially well under these conditions. The atomic fluorescence lineshape thermometry technique is quicker to perform and requires less elaborate equipment than other methods that have previously been implemented in low-pressure flames, including OH-LIF and NO-LIF. There was sufficient indium present to perform measurements at all locations in the flame, including in the pre-heat zone close to the burner plate. Two sets of temperature measurements have been independently performed by using two different diode lasers to probe two separate transitions in atomic indium. The good agreement between the two sets of data provides a validation of the technique. By comparing thermocouple profiles recorded with and without seeding of the flame, we demonstrate that any influence of seeding on the flame temperature is negligible. The overall uncertainty of the measurements reported here is estimated to be ±2.5% in the burnt gas region.

PACS 42.55.Px · 32.50.+d · 42.62.Fi

1 Introduction

It is well-known that because of the thick reaction zone prevailing in low-pressure premixed flat-flames, such flames are ideally suited for the study of flame chemistry and the validation of detailed kinetic models [1]. Reaction rates are mainly governed by temperature, so the flame temperature profile is required as an input for numerical models. Accurate temperature measurements in low-pressure flames are consequently very important to the understanding of flame chemistry. Temperature measurements are also essential for obtaining species concentrations from spectra resulting from laser induced fluorescence or optical absorption experiments, because the population in the absorbing level is a function of temperature.

Several authors have described the range of laser diagnostic techniques available for flame temperature measurement [2–4]. Notable examples include Rayleigh scattering, Raman scattering, coherent anti-Stokes Raman scattering (CARS), absorption spectroscopy, and laser induced fluorescence (LIF). These techniques are applied in the context of atmospheric pressure flames, and some are more suitable

I.S. Burns · C.F. Kaminski · J. Hult
Department of Chemical Engineering, University of Cambridge, Pembroke Street, Cambridge CB2 3RA, UK

Present address:
I.S. Burns (✉)
Department of Chemical and Process Engineering, University of Strathclyde, Montrose Street, Glasgow G1 1XJ, Scotland
e-mail: iain.burns@strath.ac.uk
Fax: +44-141-5522302

N. Lamoureux · P. Desgroux
PC2A Lille, UMR 8522, USTL, 59655 Villeneuve d'Ascq, France

C.F. Kaminski
SAOT School of Advanced Optical Technologies, Max Planck Research Group, Division III, Universität Erlangen-Nürnberg, Erlangen, Germany

than others for use in low-pressure environments. The following paragraphs give a brief summary of previous temperature measurements in low-pressure flames.

Rayleigh scattering seems to have received little attention in the context of low-pressure flame research, perhaps due to low signal levels and to the effects of elastic scattering of incident laser radiation from the surfaces of the burner chamber. In the case of Raman scattering, extremely low signal-to-noise ratios are observed at low pressure due to the low prevailing number density, meaning that thermometry is infeasible even when integration times of tens of minutes are used [5].

Vibrational N_2 CARS temperature measurements have been demonstrated in flames at a sub-atmospheric pressure of 30.0 kPa [6]. At lower pressures, however, a very much weaker signal would be detected since the CARS generation process is proportional to the square of the number density of the probed species. It is thus anticipated that N_2 vibrational CARS would not give satisfactory results at the much lower pressures usually investigated in studies of flame chemical kinetics, since the CARS signal would be several hundred times weaker than in an atmospheric pressure flame. Temperature measurements have also been performed at low pressure by rotational H_2 CARS, in a microwave-plasma diamond deposition reactor at 3.8 kPa [7], and in an oxy-acetylene diamond-formation flame at 6.7 kPa [8]. This technique was successful in these applications due to the high Raman cross-section of molecular hydrogen and to the relatively high concentrations of H_2 in the systems studied. In hydrocarbon-air flames with much lower prevailing hydrogen mole fractions, this technique is not expected to perform so well.

Methods based on absorption spectroscopy have only rarely been used for thermometry in low-pressure flames [9]. The line-of-sight absorption signal does not permit high spatial resolution to be achieved; instead a 'path-integrated' temperature is obtained which is biased by edge effects at the perimeter of the flame.

Temperature measurements in low-pressure flames have often been performed by LIF of molecules such as OH [10] and NO [5, 11]. This technique generally involves slowly tuning the wavelength of a pulsed laser over a number of individual rotational lines of the molecule of interest. The temperature is then determined by fitting a theoretical spectrum to the data, or by constructing a Boltzmann plot.

Temperature measurements by OH LIF in low-pressure flames have been implemented by various researchers [5, 10, 12–14]. A complication of the OH LIF thermometry technique is that measurement errors arise from the influence of quenching on the fluorescence quantum yield, and from the effects of rotational and vibrational energy transfer in the excited electronic state. Various possible sets of assumptions about the variation of quenching with rotational level can be used during the evaluation of temperature from OH LIF spectra. These assumptions have been considered to be limiting cases from which the range of evaluated temperatures allows a measurement uncertainty of around $\pm 5\%$ to be estimated. This can be improved upon by implementing a detailed model describing all of the energy transfer processes are accounted for [15–17], although there remains a certain degree of uncertainty in the resulting temperature measurements due to inaccuracies in the spectroscopic and collisional cross-section data.

In near-stoichiometric low-pressure flames, it is possible to measure the flame temperature profile down to below 1000 K using OH LIF thermometry [10, 12–14], although this is a rather lengthy procedure due to the time required to acquire each spectrum. The technique has also been implemented in rich flames. For example, in a $\Phi = 2.3$ propene flame at 5.0 kPa, temperature measurements based on OH LIF resulted in reasonably precise data in the burnt gases [5]. The authors reported, however, that OH LIF thermometry was only possible in the regions of the rich propene flame where the temperature was higher than 1600 K; at positions further upstream in the reaction zone, the mole fraction of OH was insufficient to give adequate LIF signal levels for temperature measurements to be possible. It has thus sometimes been necessary, especially in richer flames where the OH mole fraction is generally lower, to combine two different thermometry techniques in order to resolve the entire flame temperature profile with reasonable accuracy.

An alternative technique involves seeding mole fractions of between 0.2 and 1% of NO to low-pressure flames as a tracer for LIF thermometry. Errors due to assumptions about collisional behaviour are largely avoided in the case of NO LIF, since the quenching cross-section of the excited $A^2\Sigma^+$ $\nu' = 0$ state changes very little as a function of the rotational quantum number [18]. The NO LIF technique has also been implemented in low-pressure flames [5, 11, 19]. In their study of fuel-rich propene flames, Hartlieb et al. used multi-line NO LIF to measure temperature in the reaction zone [5], resulting in a similar precision to the OH LIF measurements performed in the burnt gases. An imaging thermometry technique based on the same principle has recently been implemented in a flame of H_2, O_2 and Ar, used in the study of nanoparticle generation [19].

In the case of seeded NO LIF, the nitric oxide reacts downstream of the flame-front in rich hydrocarbon flames, in a process known as reburning [20]. This effect becomes more pronounced as the equivalence ratio is increased [20], leading to a significant reduction in signal levels in rich flames. As a result NO LIF thermometry is often infeasible in the burnt gas region of rich hydrocarbon flames, meaning that two separate techniques must be employed in order to obtain the full temperature profile [5].

Consequently, it would be desirable to have a thermometry instrument for low-pressure flames that would allow the

entire flame temperature profile to be conveniently and accurately measured with high spatial resolution, while avoiding the use of the bulky and expensive laser systems required for molecular LIF. In this paper we report on the implementation of the diode laser induced atomic fluorescence lineshape thermometry to low-pressure flames. Diode lasers are often used to probe combustion processes by absorption spectroscopy but examples of measurements based on diode laser induced fluorescence in flames are rare. Exceptions include the use of a near-infrared diode (NIR) laser emitting at 780 nm to generate fluorescence of seeded rubidium atoms [21], and the frequency doubling of an 852 nm diode laser to perform LIF of the CH radical at 426 nm [22]. In our previous work, we have implemented laser induced fluorescence with blue extended cavity diode lasers [23, 24] and have used this to develop flame thermometry based on atomic indium [25, 26]. The initial demonstration of atomic fluorescence lineshape thermometry was made in a simple atmospheric-pressure flame [26]. Here the application of the technique is extended to the more challenging situation of the low-pressure flame.

There are several reasons for which this method should be expected to work especially well in low-pressure flames. Firstly, very strong atomic fluorescence signals can be obtained, even at seeding densities low enough to avoid appreciable absorption, since there is much less quenching than at atmospheric pressure. Secondly, at low pressure, Doppler broadening is relatively dominant over collisional broadening. This means that any slight inaccuracies in the assumptions that are made about the collisional broadening have even less impact on the measured temperature than at atmospheric pressure. Thirdly, the reactions by which indium is consumed in the flame take place much more slowly at low pressure, so the concentration of the probe species is not significantly depleted as the gases flow away from the burner plate.

2 Experimental set-up

2.1 Low-pressure burner system

Temperature measurements were performed in premixed flames of methane, oxygen and nitrogen, being burned in an enclosed stainless steel chamber at a pressure of 5.3 kPa. The flame had an equivalence ratio of 0.95, and the molar ratio N_2:O_2 was 3.5. The total volumetric flowrate of the premixed gases was 4.5 slpm. The water-cooled burner consisted of a flat metal plate drilled with 800 μm capillary holes, which were regularly distributed over a circular region of 63 mm diameter. The burner chamber was equipped with two small windows at opposite sides, through which the laser beam passed. On a perpendicular axis, there were two larger windows, one of which was used to collect the fluorescence signal. It was possible to translate the burner head vertically with respect to the chamber and the height of the measurement volume above the burner surface was accurately measured.

The flows of gases were regulated by mass flow controllers (TYLAN FC260). The nitrogen flow was divided between two separate mass flow controllers. A trace quantity of atomic indium was added to the flame by passing one of the two N_2 streams through a spray-type nebuliser containing an aqueous solution of indium chloride ($InCl_3$) with a concentration of roughly 0.13 M. The flowrate of nitrogen through the nebuliser and the concentration of the solution were adjusted to give a level of indium seeding that, while allowing for a strong LIF signal, was low enough to give negligible fractional absorption of the incident laser beam by indium.

The capacity of the reservoir in the nebuliser was about 10 ml and it took approximately 2 hours for this volume of liquid to be depleted. The seeding process thus led to a modification in the concentrations in the pre-mixed gas stream, with approximately 0.1 slpm of water vapour being added. This mole fraction of about 2% water vapour in the premixed gases is much greater than has been typical in the atomic fluorescence measurements that we have previously performed at atmospheric pressure [25, 26]. Steps were therefore taken to confirm that this addition of water was not sufficient to perturb significantly the flame conditions. This was done by performing thermocouple measurements of the flame temperature profile, both in the presence and absence of seeding (see Sect. 2.3). The good precision of the thermocouple measurements makes them well-suited to distinguish any temperature difference between these two situations. In spite of this statistical reproducibility, thermocouple measurements are characterised by a systematic uncertainty generally considered to be in the region of at least ±100 K, even after all correction procedures have been implemented, so the atomic fluorescence method presented here is thought to be appreciably more accurate.

2.2 Temperature measurements using diode laser atomic fluorescence

Two separate extended cavity diode lasers emitting at around 410.2 nm and around 451.1 nm, respectively, [27] were used to probe the $5^2P_{1/2} \rightarrow 6^2S_{1/2}$ and $5^2P_{3/2} \rightarrow 6^2S_{1/2}$ transitions of atomic indium. The lineshapes of the resulting LIF spectra were used to make two independent temperature measurements at a range of locations in the flame. The experimental technique was similar to that reported previously [26], so only a brief description is given here; the set-up is shown in Fig. 1. The same experimental procedure was followed in the case of each of the two extended cavity diode lasers that were employed. The correct

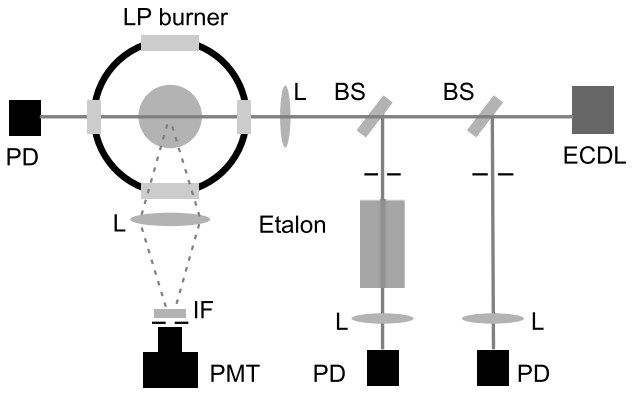

Fig. 1 Optical set-up for the atomic fluorescence measurements. ECDL: extended-cavity diode laser; BS: beam-splitter; L: lens; PD: photodiode; IF: interference filter; PMT: photomultiplier tube

wavelength was roughly found using a low-resolution fibre-coupled spectrometer (OceanOptics USB4000); further adjustment was then done to tune to the absorption line of an indium hollow cathode lamp (Hereaus).

An etalon was used to ensure that the laser operated on a single longitudinal mode over its scan range, and to permit correction for any slight non-linearities in the wavelength tuning. The laser intensity was recorded by a reference photodiode so that the fluorescence spectra could be normalised for laser power variation. The laser beam was focussed at the central vertical axis of the burner and the resulting fluorescence signal collected by imaging through a pin-hole and an interference filter ($\lambda_c = 451.1$ nm; $\Delta\lambda = 3$ nm) onto a photomultiplier tube. The measurement volume was defined by a cylinder roughly 100 µm in diameter and 800 µm in length, with the long axis parallel to the burner surface. A much shorter measurement volume could have been obtained, if necessary, by use of a smaller pin-hole. The intensity of the laser beam transmitted through the burner was also recorded to confirm that any attenuation of the laser due to absorption by indium atoms was negligible. The signals were pre-amplified (bandwidth = 20 kHz), before being digitised and stored by an oscilloscope. Measurements were made with each laser for a range of heights above the burner. For every measurement location, 200 single-scan spectra were recorded. The linear proportionality of the LIF signal to the incident laser power was experimentally confirmed by performing an excitation power scan.

The processing of the experimental data involved the determination of the temperature based on the spectral shape. A similar procedure was followed in the case of both the $5^2P_{1/2} \rightarrow 6^2S_{1/2}$ and $5^2P_{3/2} \rightarrow 6^2S_{1/2}$ indium transitions. The raw experimental data for each temperature measurement consisted of four parameters measured during the wavelength scan: the reference power trace, the transmitted power trace, the etalon transmission, and the fluorescence trace. Examples of these raw data traces after background

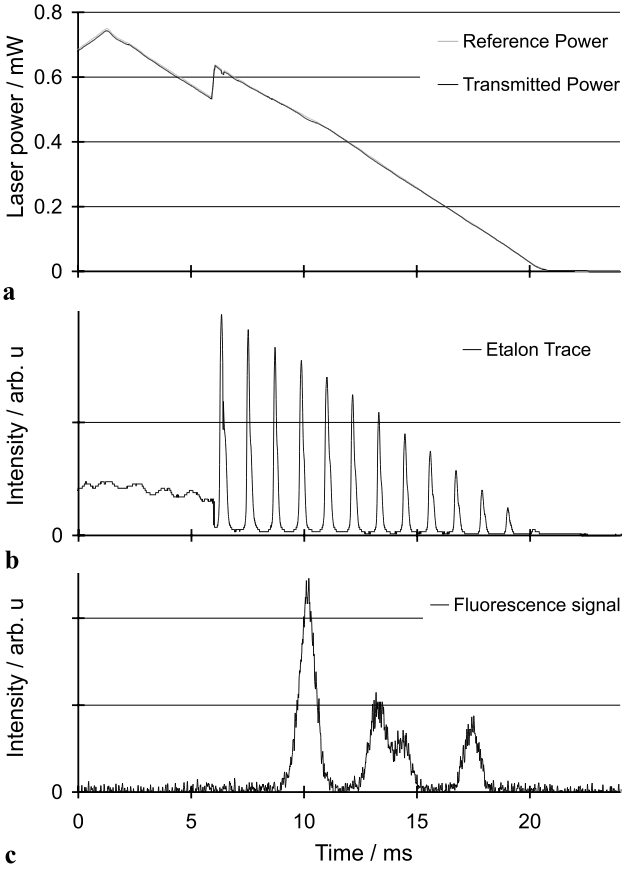

Fig. 2 Examples of raw data traces (after background subtraction) for a single wavelength-scan of the 410.2 nm diode laser probing the $5^2P_{1/2} \rightarrow 6^2S_{1/2}$ indium transition. (**a**) Reference laser power and transmitted laser power (these lie very close together so are indistinguishable); (**b**) etalon trace; (**c**) fluorescence signal

subtraction are shown in Fig. 2. The background levels to be subtracted from each of the traces were estimated by taking the average values of the signals in a region of the scan where the laser current was below the threshold for lasing (after 21 ms in Fig. 2(a)). This eliminates the need to separately record background signal levels. An accurate calibration of the photodiode readings had been made through comparison to absolute laser power measurements made using a thermopile powermeter.

For each temperature evaluation, a theoretical fit was made to an average of 200 individual normalised fluorescence spectra. In the present study, this data processing was performed after all of the experiments were completed but real-time analysis would also be feasible. The floating parameters in the fit were: position of the first hyperfine peak; intensity of first hyperfine peak; temperature; background offset. The fitted function was a sum of Voigt profiles, one for each hyperfine line of the transition. The hyperfine structures of the probed transitions are well known [28]. The Doppler component of the Voigt profile was calculated in the fitting routine from the temperature. The Lorentzian com-

ponent, $\Delta\nu_L$, comprises the sum of collisional broadening, $\Delta\nu_C$, and natural broadening, $\Delta\nu_N$. Of these contributions, $\Delta\nu_C$ was at least twenty times larger than $\Delta\nu_N$ for the conditions investigated during the present study, and natural broadening is therefore a small correction whose omission would lead to an error in the measured temperature of around 25 K or less. The collisional broadening parameter, $\Delta\nu_C$, was calculated from temperature and pressure, using the impact broadening approximation [29] to infer an exponent of 0.7 for the temperature dependence:

$$\Delta\nu_C = \Delta\nu_C^{\mathrm{ref}} \left(\frac{T^{\mathrm{ref}}}{T}\right)^{0.7} \left(\frac{p}{p^{\mathrm{ref}}}\right). \quad (1)$$

The impact broadening assumption is valid in cases when the duration of collisions is much shorter than the time between collisions [29]. It is thus especially applicable at atmospheric pressure and below, since the mean free path is several orders of magnitude greater than the atomic diameter.

A reference point $\Delta\nu_C^{\mathrm{ref}}(T^{\mathrm{ref}}, p^{\mathrm{ref}})$ is required for use of the above expression. For this purpose, we used the values that were measured previously in the burnt gas region of an atmospheric-pressure stoichiometric flame of methane and air [26]. These lead to reference broadening parameters of $\Delta\nu_C^{\mathrm{ref}}(5^2P_{1/2} \rightarrow 6^2S_{1/2}) = 4.99$ GHz, and $\Delta\nu_C^{\mathrm{ref}}(5^2P_{3/2} \rightarrow 6^2S_{1/2}) = 4.78$ GHz; the reference temperature, $T^{\mathrm{ref}} = 2200$ K, had been established by independent measurement techniques [26]. It is acceptable to use a reference measurement taken at a pressure relatively far from the conditions of the present experiment since, at atmospheric pressure and below, the collision frequency is a linear function of pressure. Furthermore, as discussed further in Sect. 3.2, small errors in the value of $\Delta\nu_C$ would have only a very slight influence on the evaluated temperature for a low-pressure flame.

To demonstrate the sensitivity of the transition lineshapes to temperature at low-pressure conditions (5.3 kPa), simulated spectra for the two transitions are shown in Fig. 3 for temperatures of 1000 and 1800 K. The spectra were calculated using a sum of Voigt profiles representing the hyperfine components of the transitions. The Lorentzian component of the Voigt profile was calculated using (1) together with the reference data specified above. The positions and relative intensities of the hyperfine components of each transition are shown by the solid vertical lines in Fig. 3. The spacings of the hyperfine lines for the two transitions probed are given in the literature [28], and the theoretical relative intensities can be calculated from a simple formula involving the F, J and I quantum numbers [30]. In the case of the $5^2P_{1/2} \rightarrow 6^2S_{1/2}$ transition, shown in Fig. 3(a), there are four hyperfine components. In contrast to the atmospheric pressure fluorescence spectra that we have presented previously [26], the individual hyperfine lines are clearly visible

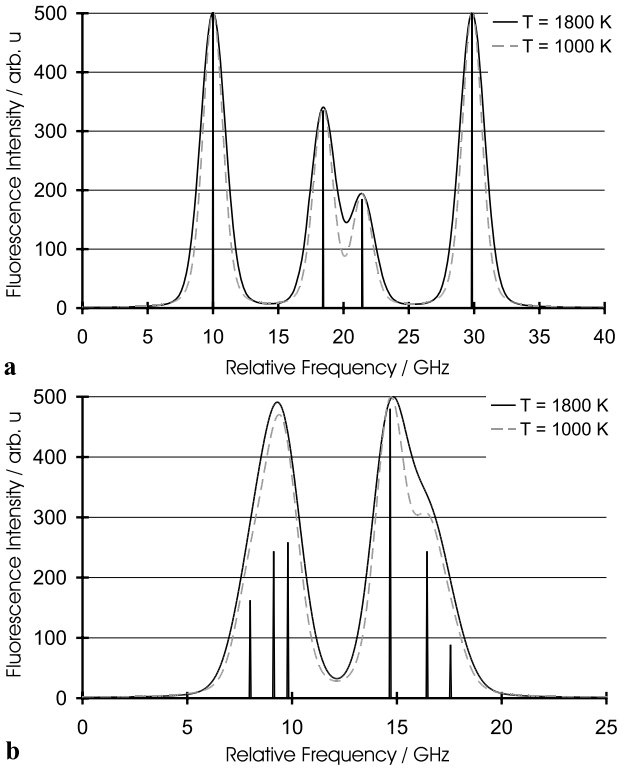

Fig. 3 Simulated fluorescence spectra of atomic indium at a pressure of 5.3 kPa, for temperatures of 1000 and 1800 K. (**a**) The $5^2P_{1/2} \rightarrow 6^2S_{1/2}$ transition (410.2 nm); (**b**) the $5^2P_{3/2} \rightarrow 6^2S_{1/2}$ transition (451.1 nm). The spectra are normalised to have the same maximum value. The positions and relative intensities of the hyperfine lines are indicated by the *solid vertical lines*

in this low-pressure spectrum. The $5^2P_{3/2} \rightarrow 6^2S_{1/2}$ transition, shown in Fig. 3(b), has six hyperfine components consisting of two groups of three closely spaced lines. These two groups of lines appear as two separate features on the spectrum shown here.

It can be seen from Fig. 3 that, as temperature is increased, the individual hyperfine lines become broader. This allows the flame temperature to be determined based on atomic fluorescence spectra by performing a non-linear least squares fit of the modelled lineshape to the experimental data. The atomic fluorescence lineshapes are most sensitive to temperature in regions where there is a dip between two adjacent hyperfine lines. At the conditions of interest in the present study, we see from Fig. 3(a) that such a dip exists for the $5^2P_{1/2} \rightarrow 6^2S_{1/2}$ transition at 20 GHz on the relative frequency scale, and from Fig. 3(b) that a similar trough exists at around 16 GHz for the $5^2P_{3/2} \rightarrow 6^2S_{1/2}$ transition. It is thought that the presence of hyperfine lines whose spacing leads to dips with depth sensitive to temperature allows for more accurate thermometry than would be possible by fitting to an isolated line.

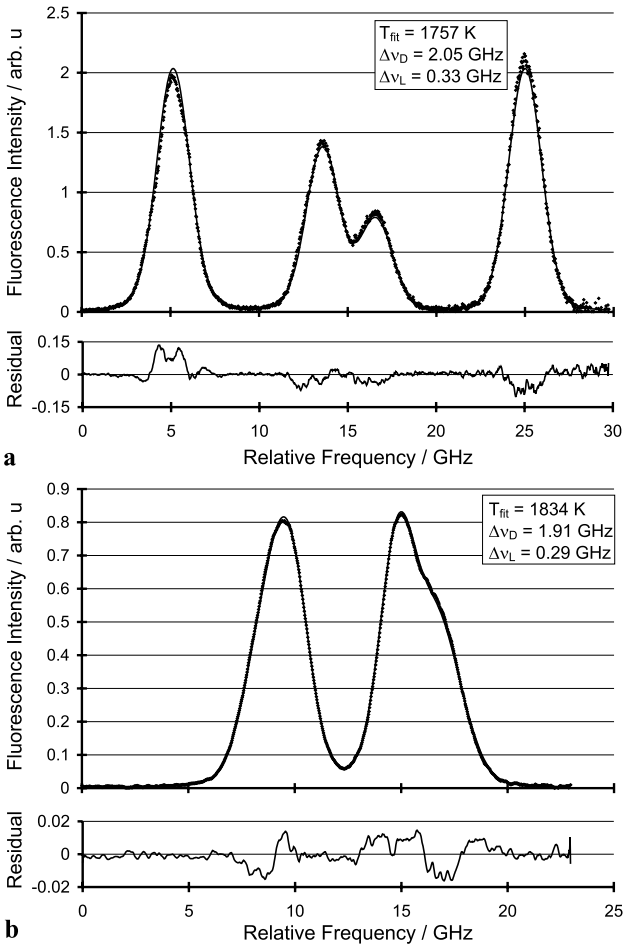

Fig. 4 Experimental fluorescence spectra (*dots*) for atomic indium with theoretical fits (*solid lines*). (**a**) The $5^2P_{1/2} \rightarrow 6^2S_{1/2}$ transition (410.2 nm); (**b**) the $5^2P_{3/2} \rightarrow 6^2S_{1/2}$ (451.1 nm). The spectra shown here were recorded at a height of 18 mm above the burner surface

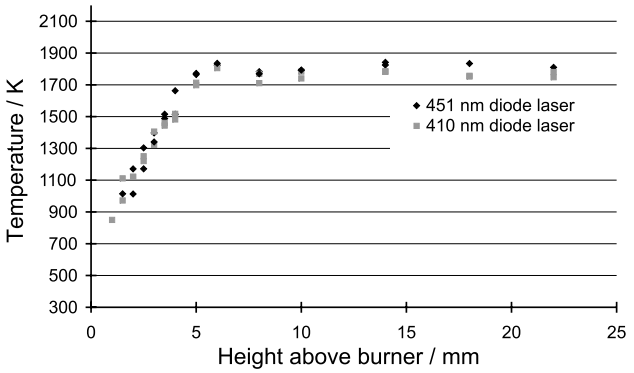

Fig. 5 Flame temperatures measured using atomic fluorescence lineshapes

2.3 Temperature measurements by thermocouple

Temperature profiles were also measured using a Pt-30%Rh-/Pt-6%Rh thermocouple with a junction diameter of around (300 μm) coated to reduce catalytic effects. The stirrup-shaped thermocouple was positioned parallel to the burner surface with the junction placed at its central vertical axis. Radiation losses were corrected for using a standard electric compensation technique. Despite these careful procedures, the global accuracy of such thermocouple measurements is thought to be at least ±100 K in the burnt gases.

3 Results

3.1 Low-pressure atomic LIF spectra

Shown in Fig. 4 are examples of spectra recorded in the burnt gas region of the flame (18 mm above the burner) for the $5^2P_{1/2} \rightarrow 6^2S_{1/2}$ indium transition at 410.2 nm, and the $5^2P_{3/2} \rightarrow 6^2S_{1/2}$ transition at 451.1 nm. The experimental data are shown together with a fitted spectrum, and the residual is shown on a separate axis. The good agreement between experiment and theory leads to the possibility of accurate and precise temperature measurements. The residuals between the experimental and theoretical spectra are very small and are thought to result from slight random artefacts in the experimental data, whose overall effect on the measurement is small as shown by the favourable precision of the temperature measurements shown below.

Temperatures were evaluated from the theoretical fits to the experimental spectra, and are shown in Fig. 4 along with the corresponding broadening parameters. In the case of the $5^2P_{1/2} \rightarrow 6^2S_{1/2}$ transition shown in Fig. 4(a), similar temperatures are obtained regardless of whether a fit is made to the full spectrum (as shown), or to the region of the central two hyperfine peaks only. This supports the idea that the temperature sensitivity derives from the dip between the adjacent hyperfine peaks.

Although at extremely low pressure it is possible to measure temperature based on fitting of pure Doppler profiles (demonstrated for example in a hollow cathode lamp by absorption spectroscopy of aluminium atoms [31]), at the flame pressure of 5.3 kPa in the present work it was essential to include the relatively small Lorentzian component to achieve good spectral fits. It was found that a fitting procedure based on a sum of pure Doppler profiles resulted in somewhat poorer agreement with the experimental spectra, especially in the line wings, and that this caused substantial over-prediction of the flame temperature. The full Voigt profile model was therefore used in the evaluation of all of the temperature data reported here.

3.2 Flame temperature profile

The resulting temperature measurements are shown in Fig. 5. Measurements were made at heights of between

1 and 22 mm above the burner surface. The measured gas temperature rises to a maximum of around 1800 K. After reaching this value at around 6 mm above the burner, there is a plateau where the temperature stays roughly constant. The mean temperature measured in the burned gas region using the 410.2 nm diode laser was 1765 K, while the corresponding value evaluated using the 451.1 nm laser data was 1810 K.

4 Discussion

An important point to note is that the temperature profiles measured independently with the two different lasers are in good agreement with each other, both in terms of the shape of the temperature profile and the absolute values. The proximity of these results lends weight to the validity of the technique described here.

In the case of both lasers, the measurements in the region of the plateau have a standard deviation of ±25 K, and this figure thus represents an upper estimate of the precision in the burnt gas region. In addition to the consideration of precision, it is also necessary to discuss possible sources of systematic inaccuracy, whereby the result could be biased in a manner that is not reduced by averaging of repeated measurements. One source of error would be the modelling of the Lorentzian component of the spectral profile. The reference broadening values used in (1) are known with an uncertainty of ±2.5%. By making spectral fits to the data using adjusted values of $\Delta\nu_C^{\mathrm{ref}}$, it was found that this would lead to a possible error of approximately ±15 K in measured temperature in the low-pressure flame. Further to this, the influence of inelastic collisions on the Lorentzian width must be considered. Inelastic collisions have a minor contribution to the overall Lorentzian width [29], and are neglected in (1). Even based on an upper estimate of the possible influence of inelastic collisions, we predict that they would have a negligible contribution to the uncertainty in the burnt gas region but could give rise to an error in temperature of around ±20 K further down in the reaction zone, where the flame temperature and composition are further from those of the reference measurement.

A second type of systematic error results from a possible influence of the seeding process on the flame temperature, which we investigated by performing thermocouple measurements. Temperature profiles measured by thermocouple both in the presence and absence of seeding are presented in Fig. 6. It is evident that the seeding does not significantly influence the flame temperature, the largest discrepancy between the two thermocouple traces being around 20 K at the location of the flame front. This conclusion was confirmed by calculation of the adiabatic flame temperature showing

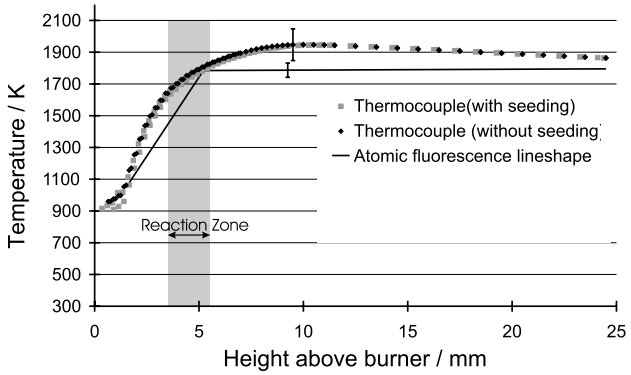

Fig. 6 Thermocouple measurements in the presence and absence of seeding. Atomic fluorescence lineshape temperature data are also shown as a *line* fitted through the data. Also shown is the approximate location of the reaction zone, according to chemiluminescence data

that a presence of about 2% vol. water vapour in the premixed gases would lead to a reduction in the burnt gas temperature of approximately 18 K. This small uncertainty was added to the error resulting from the modelling of the lineshape mentioned above. It is quite likely that the seeding may influence properties of the flame other than temperature, such as species concentration profiles. These effects are of little interest though, since the seeding is performed only while the temperature measurements are done and other parameters would be measured without seeding.

Taking account of precision and systematic inaccuracy, the overall uncertainty in the individual temperature measurements in the burnt gas region is approximately ±2.5% (±45 K), which confirms the suitability of this thermometry technique in low-pressure flames. It is thought that this uncertainly could be reduced still further by repeating the measurement of the temperature profile several times, thus improving the precision. This would be readily feasible since the entire temperature profile of the flame can be recorded with a single laser in roughly one hour, compared to tens of minutes for an individual temperature measurement at one point in the flame using a scanned-dye-laser LIF approach.

The difference between the mean temperatures measured in the burned gases with the two diode lasers was 45 K. This is at the upper range of what might be expected based on the estimated measurement uncertainty, but is quite feasible if the measurements with the two lasers should happen to have small systematic errors in opposite directions.

Also included in Fig. 6 is a line showing the temperature measurements based on atomic fluorescence lineshapes. This was obtained by making linear fits to the temperature data in the burnt gases, and in the region of the steep gradient. Comparison of the thermocouple profile shown in to the atomic LIF temperature profile reveals that the shapes of the profiles are somewhat different: the temperature profile measured by thermocouple does not show a plateau, but reaches

a maximum before gradually declining. This means that the difference between the two techniques is greatest where the thermocouple temperature is at its maximum. As we have already noted, the type of thermocouple technique employed here is considered to have a measurement inaccuracy of at least ± 100 K, due to uncertainties in the radiation correction procedure and various other error sources. It should be noted that the main objective of the thermocouple measurements reported here was to demonstrate that any influence of the indium seeding on the flame properties is very small.

5 Conclusions

Diode laser induced fluorescence lineshape thermometry has been implemented in low-pressure flames and shown to work especially well in such systems. This represents a challenging application of the measurement in a system that is of practical interest for studies of flame chemistry. The technique is based on analysis of atomic fluorescence spectra, generated using low-power diode lasers. This allows for a relatively inexpensive and compact measurement tool, while offering favourable precision and accuracy with good spatial resolution and a short acquisition-time. The particular considerations related to the implementation at low pressure, including aspects related to the lineshape modelling were emphasised. The influence of seeding of the flame on the temperature profile was considered and shown to be negligible. A thorough analysis of error sources resulted in an estimated uncertainty of ± 45 K in the burnt gas zone. The two independent flame temperature profiles obtained by using two blue diode lasers to probe two separate transitions of atomic indium show good agreement. Although two lasers were used in this experiment for the purpose of this cross-comparison, future implementations would of course only require a single laser to be used.

Acknowledgements ISB was supported by a Research Fellowship from St. John's College, Cambridge, UK. This work was funded by the Royal Society, UK, and partially by the EPSRC (Engineering and Physical Sciences Research Council, UK). Bilateral travelling expenses were provided by a grant from the Alliance Franco-British Partnership Programme administered by the British Council. CFK is grateful to the Leverhulme Trust for personal sponsorship, and JH acknowledges support by an Advanced Research Fellowship (EP/C012399/1) from the EPSRC.

References

1. J. Vandooren, J. Bian, Proc. Combust. Inst. **23**, 341 (1990)
2. A.C. Eckbreth, *Laser Diagnostics for Combustion Temperature and Species* (Gordon & Breach, Amsterdam, 1996)
3. N.M. Laurendeau, Prog. Energy Combust. Sci. **14**, 147 (1988)
4. W.P. Stricker, in *Applied Combustion Diagnostics*, ed. by K. Kohse-Höinghaus, J.B. Jeffries (Taylor & Francis, London, 2002)
5. A.T. Hartlieb, B. Atakan, K. Kohse-Höinghaus, Appl. Phys. B **70**, 435 (2000)
6. D. Bradley, M. Lawes, M.J. Scott, N. Usta, Combust. Flame **124**, 82 (2001)
7. C.F. Kaminski, P. Ewart, Appl. Phys. B **64**, 103 (1997)
8. S. Roy, W.D. Kulatilaka, R.P. Lucht, N.G. Glumac, T. Hu, Combust. Flame **130**, 261 (2002)
9. R.G. Daniel, K.L. McNesby, A.W. Miziolek, Appl. Opt. **35**, 4018 (1996)
10. K.J. Rensberger, J.B. Jeffries, R.A. Copeland, K. Kohse-Höinghaus, Appl. Opt. **28**, 3556 (1989)
11. M. Tamura, J. Luque, J.E. Harrington, P.A. Berg, G.P. Smith, J.B. Jeffries, D.R. Crosley, Appl. Phys. B **66**, 503 (1998)
12. P. Desgroux, L. Gasnot, J.F. Pauwels, L.R. Sochet, Appl. Phys. B **61**, 401 (1995)
13. X. Mercier, L. Pillier, A. El Bakali, M. Carlier, J.F. Pauwels, P. Desgroux, Faraday Discuss. **119**, 305 (2001)
14. L. Pillier, A. El Bakali, X. Mercier, A. Rida, J.F. Pauwels, P. Desgroux, Proc. Combust. Inst. **30**, 1183 (2005)
15. R. Kienle, M.P. Lee, K. Kohse-Höinghaus, Appl. Phys. B **62**, 583 (1996)
16. U. Rahmann, W. Kreutner, K. Kohse-Höinghaus, Appl. Phys. B **69**, 61 (1999)
17. A. Brockhinke, W. Kreutner, U. Rahmann, K. Kohse-Höinghaus, T.B. Settersten, M.A. Linne, Appl. Phys. B **69**, 477 (1999)
18. W.G. Bessler, C. Schulz, Appl. Phys. B **78**, 519 (2004)
19. H. Kronemayer, P. Ifeacho, C. Hecht, T. Dreier, H. Wiggers, C. Schulz, Appl. Phys. B **88**, 373 (2007)
20. B. Atakan, A.T. Hartlieb, Appl. Phys. B **71**, 697 (2000)
21. P.E. Walters, T.E. Barber, M.W. Wensing, J.D. Winefordner, Spectrochim. Acta Part B **46**, 1015 (1991)
22. K.A. Peterson, D.B. Oh, Opt. Lett. **24**, 667 (1999)
23. J. Hult, I.S. Burns, C.F. Kaminski, Opt. Lett. **29**, 827 (2004)
24. I.S. Burns, J. Hult, C.F. Kaminski, Appl. Phys. B **79**, 491 (2004)
25. J. Hult, I.S. Burns, C.F. Kaminski, Proc. Combust. Inst. **30**, 1535 (2005)
26. I.S. Burns, J. Hult, G. Hartung, C.F. Kaminski, Proc. Combust. Inst. **31**, 775 (2007)
27. J. Hult, I.S. Burns, C.F. Kaminski, Appl. Opt. **44**, 3675 (2005)
28. G.V. Deverall, K.W. Meissner, G.J. Zissis, Phys. Rev. **91**, 297 (1953)
29. A.P. Nefedov, V.A. Sinel'shchikov, A.D. Usachev, Phys. Scr. **59**, 432 (1999)
30. C. Candler, *Atomic Spectra and the Vector Model* (Hilger, London, 1964)
31. H. Scheibner, S. Franke, S. Solyman, J.F. Behnke, C. Wilke, A. Dinklage, Rev. Sci. Instrum. **73**, 378 (2002)